Published online 25 July 2010 *Nucleic Acids Research, 2010, Vol. 38, No. 21* ***7611–7625***
doi:10.1093/nar/gkq651

Genetic and functional interactions between Mus81–Mms4 and Rad27

Min-Jung Kang, Chul-Hwan Lee, Young-Hoon Kang, Il-Taeg Cho, Tuan Anh Nguyen and Yeon-Soo Seo*

Center for DNA Replication and Genome Instability, Department of Biological Sciences, Korea Advanced Institute of Science and Technology, Daejeon, 305-701, Korea

Received June 6, 2010; Revised July 6, 2010; Accepted July 7, 2010

ABSTRACT

The two endonucleases, Rad27 (yeast Fen1) and Dna2, jointly participate in the processing of Okazaki fragments in yeasts. Mus81–Mms4 is a structure-specific endonuclease that can resolve stalled replication forks as well as toxic recombination intermediates. In this study, we show that Mus81–Mms4 can suppress *dna2* mutational defects by virtue of its functional and physical interaction with Rad27. Mus81–Mms4 stimulated Rad27 activity significantly, accounting for its ability to restore the growth defects caused by the *dna2* mutation. Interestingly, Rad27 stimulated the rate of Mus81–Mms4 catalyzed cleavage of various substrates, including regressed replication fork substrates. The ability of Rad27 to stimulate Mus81–Mms4 did not depend on the catalytic activity of Rad27, but required the C-terminal 64 amino acid fragment of Rad27. This indicates that the stimulation was mediated by a specific protein–protein interaction between the two proteins. Our *in vitro* data indicate that Mus81–Mms4 and Rad27 act together during DNA replication and resolve various structures that can impede normal DNA replication. This conclusion was further strengthened by the fact that *rad27 mus81 or rad27 mms4* double mutants were synergistically lethal. We discuss the significance of the interactions between Rad27, Dna2 and Mus81–Mms4 in context of DNA replication.

INTRODUCTION

During the replication of chromosomal DNA, replication forks (RFs) are likely to encounter many potential obstacles such as damaged lesions or tightly bound proteins, resulting in the formation of stalled or collapsed RFs. In order to maintain genome stability, cells have developed mechanisms to reestablish impaired RFs. One mechanism contributing to RF restart is homologous recombination, which requires multiple enzymatic activities (1,2). When progression of RFs is blocked, they regress and form a Holliday junction (HJ)-like structure that arises from the annealing of regressed leading and lagging strands (1,3).

Collapsed or regressed RFs must be processed to restart DNA replication, and can be restored with the aid of RecQ-family helicases, which include Sgs1 (budding yeast), Rqh1 (fission yeast), BLM, WRN and RTS (humans) helicases (4). They promote reversion of regressed RFs (4–6). The heterodimeric Mus81–Mms4 complex has been implicated in processing of stalled and blocked RFs as well as in the processing of recombination intermediates (2,7,8). Mus81–Mms4 is a structure-specific endonuclease originally identified in a *sgs1* synthetic-lethal screen as a component that acts in parallel or redundant pathways with Sgs1 (9–16). *In vitro* experiments showed that the Mus81–Mms4 complex cleaved nicked Holliday junctions, D loop, RFs, and 3′ flaps that could form *in vivo* during the repair of damaged RFs (11,12,14–16). The common structural feature of Mus81–Mms4 substrates is the presence of three- or four-way junctions containing a 5′ end at the junction, which serves to direct the cleavage reaction by Mus81–Mms4 (9,11,12,17,18). Furthermore, *mus81* mutants exhibited hypersensitivity to methyl methanesulfonate (MMS), cisplatin, hydroxyurea (HU) and UV, all of which can lead to either the stalling or the collapse of RFs (19–23). In general, inactivation of genes involved in fork processing displayed several types of genome instability, such as increased rates of both mitotic and meiotic recombination, gross chromosomal rearrangements and chromosome loss (4,5,24–27). Thus, failure to repair impaired RFs puts cells at high risks of genome instability, contributing in part to the development of human diseases such as cancers (4). In humans,

*To whom correspondence should be addressed. Tel: +82 42 350 2637; Fax: 82 42 350 2610; Email: yeonsooseo@kaist.ac.kr

Bloom syndrome, Werner syndrome and Rothmund–Thomson syndrome are caused by mutations in the BLM, WRN and RTS genes, respectively.

Flap endonuclease 1 (Fen1) is another structure-specific endonuclease that resolves single-stranded flap DNA intermediates. With this activity, it participates in virtually all DNA transactions such as DNA replication, repair and recombination (28–30). In addition, many proteins interact functionally and genetically with Fen1 (29). During DNA replication, Fen1 is required to quantitatively remove the RNA primer in Okazaki fragments (28–30). RNase H, which can remove most of the initiator RNA endonucleolytically, leaves one ribonucleotide residue upstream of the RNA–DNA junction. The removal of the last ribonucleotide requires Fen1 exonuclease activity (28,30). Alternatively, Fen1 can cleave a 5′ flap containing RNA–DNA generated by DNA polymerase (pol) δ strand displacement activity, to directly generate ligatable nicks. In this case, the entire RNA primer can be removed in the absence of RNase H activity (28,30). When a flap is long enough to be coated with replication protein A (RPA), Dna2 endonuclease activity becomes essential because the RPA-coated flaps are resistant to Fen1 activity, but stimulate Dna2-catalyzed cleavage. Such processing events generate short flaps devoid of RPA, which can be processed rapidly by Fen1 (31). Thus, RPA provides a mechanism by which the processing of flaps can switch from Dna2 to Fen1 (31). The concerted action of Dna2 and Fen1 efficiently generates nicks that can be sealed by DNA ligase 1 (31).

It is worthwhile to mention that *MUS81* or *MMS4* interacted genetically with several genes involved in DNA replication. For example, deletion of *RNH202* (a subunit of RNase H2) in a *mus81* background increased its sensitivity to camptothecin and to HU, while these drugs had no significant effect on *rnh202*Δ alone (32). This result suggests that RNase H2 and Mus81–Mms4 act in parallel to overcome camptothecin- and HU-induced DNA damage. Furthermore, *rad27*Δcells lacking yeast Fen1 (yFen1) suffer severe synthetic growth defects or lethality in combination with mutations in *mus81* or *mms4* (33). Both RNase H2 and Fen1 are known to play critical roles in processing of Okazaki fragments in eukaryotes. However, the manner in which Mus81–Mms4 participates in Okazaki fragment processing is presently unclear. In this report, we have investigated functional and physical interactions between Dna2, Fen1 and Mus81–Mms4. Our findings indicate that Mus81–Mms4 and Rad27 act together via direct interactions during processing of Okazaki fragments and resolution of damaged RFs.

MATERIALS AND METHODS

Enzymes, antibodies, DNA and nucleotides

Oligonucleotides used in this study were commercially synthesized by Genotech (Daejeon, Korea) and their sequences are listed in Table 1. All oligonucleotides were gel-purified prior to use. Nucleoside triphosphates were obtained from Sigma-Aldrich, and [γ-^{32}P] adenosine triphosphates (ATP) (>5000 Ci/mmol) was purchased from IZOTOP (Budapest, Hungary). Restriction endonucleases and polymerase chain reaction (PCR) polymerases were purchased from either New England Biolabs (Beverly, MA) or Enzynomics (Daejeon, Korea). The pRS plasmids were purchased from New England Biolabs. The pET28 vectors used for protein expression in *Escherichia coli* were from Novagen (Darmstadt, Germany). Isopropyl β-D-1-thiogalactopyranoside (IPTG) and X-gal were from ElpisBiotech (Daejeon, Korea). Imidazole was from Acros Organics (Geel, Belgium). The uracil analog, 5-fluoroorotic acid (5-FOA) was obtained from Duchefa Biochemie (Haarlem, Netherland). Antibodies used for immunoprecipitation or western blotting were obtained from; anti-His (Qiagen, Valencia, CA, USA), PAP (an antibody:peroxidase conjugate, Sigma-Aldrich), and anti-FLAG (Sigma-Aldrich).

Preparation of substrates

The DNA substrates used in this study included 3′ flap (3′F), RF, RF leading strand regressed (RLe), nicked Holliday junction (nHJ) and 5′ double flap (5′DF). DNA substrates for nucleases were prepared using the synthetic oligonucleotides listed in Table 1. The oligonucleotides used to construct DNA substrates are indicated in each figure with encircled numbers at their schematic structure. Briefly, one of the three or four strands (10 pmol) was first 5′-end labeled with [γ-^{32}P]

Table 1. Oligonucleotides used to construct DNA substrates in this study

No.	Nucleotide sequences (length in nt)
1	5′-GAAAACATTATTAATGGCGTCGAGCGTCCGTAGGCACAAGGCGAACTGCTAACGG-3′ (55)
2	5′-CCGTTAGCAGTTCGCCTTGTGCCTATTTTTTTTTTTTTTTTTTTT-3′ (45)
3	5′-CGGACGCTCGACGCCATTAATAATGTTTTC-3′ (30)
4	5′-CGAACAATTCAGCGGCTTTAACCGGACGCTCGACGCCATTAATAATGTTTTC-3′ (52)
5	5′-GAAAACATTATTAATGGCGTCGAGCTAGGCACAAGGCGAACTGCTAACGG-3′ (50)
6	5′-CGCATCCTATCAGTTCGTATGCAGTGTCCGGTTAAAGCCGCTGAATTGTTCG-3′ (52)
7	5′-ACTGCATACGAACTGATAGGATGCG-3′ (25)
8	5′-GAAAACATTATTAATGGCGTCGAGC-3′ (27)
9	5′-CCGTTAGCAGTTCGCCTTGTGCCTA-3′ (25)
10	5′-CCGTTAGCAGTTCGCCTTGTGCCTAG-3′ (26)
11	5′-GCTTTAACCGGACGCTCGACGCCATTAATAATGTC-3′ (38)

ATP (10 pmol) by polynucleotide kinase according to the manufacturer's protocol. The labeled oligonucleotides were then annealed to other oligonucleotides (20 pmol) in buffer (5 mM HEPES-NaOH/pH7.5, 300 mM NaCl) using a PCR machine (95°C for 5 min, 65°C for 30 min and −0.5°C/min to 25°C). All annealed substrates were purified by 10% polyacrylamide gel electrophoresis (PAGE) prior to use.

Multi-copy suppression of *dna2K1080E* lethality

The plasmid pRS325-*MUS81*/*MMS4* was transformed into yJA1B+JK65 (*MATα ade2-101 ura3-52 lys2-801 trpΔ63 his3-Δ200 leu2-Δ1 GAL*$^+$ *dna2Δ::HIS3*) harboring both pRS316-*DNA2* and pRS314-*dna2K1080E*. In pRS325-*MUS81*/*MMS4*, expression of Mus81 and Mms4 proteins were driven by their native promoters. The transformants were grown on SD-His-Trp-Leu plates. Single colonies from transformants were grown in liquid media, and the cells were spotted in 10-fold serial dilutions onto SD-His-Trp-Leu plates with or without 5-fluoroorotic acid (5-FOA). The plates were incubated for 3 days at 30°C. Loss of pRS316-*DNA2* in the presence of 5-FOA in the media allowed us to measure whether the expression of Mus81–Mms4 (in pRS325) suppressed the *dna2K1080E* mutant allele (in pRS314).

Construction of expression vectors

All recombinant proteins were expressed as native or fusion proteins in *E. coli* by the use of the pET21c and pET28a (Novagen). Constructions of all expression vectors were performed similarly as follows: PCR fragments were obtained with appropriate pairs of primers, and amplified fragments were purified using QIA-quick gel extraction kit (Qiagen). All fragments amplified contained a unique restriction site at each end to allow directional cloning into a relevant vector. The authenticity of all constructed plasmids was confirmed by sequencing inserted DNA fragments. In order to produce hexahistidine-tagged Mms4 at its N-terminus, for example, a pair of primers, 5′-GAA TTC ATG AGC CG ATC GTT GAT-3′ and 5′-ACG CGT CGA CTC ATT CAA TAG TAT CAT T-3′ (EcoRI and SalI sites used for cloning are underlined, respectively) were used to amplify the *MMS4* gene with yeast genomic DNA as template. The amplified fragments were digested with EcoRI and SalI, and cloned into pET28a cleaved with EcoRI and SalI, generating pET-His$_6$-Mms4. The pET-Mus81 was prepared by the use of 5′-GGA ATT CCA TAT GGA ACT CTC ATC AAA C-3′ and 5′-GCG GCC GCC TA AGT TTA CCA AAA GC (NdeI and NotI site, respectively). The amplified fragments were then cloned into NdeI and NotI sites of pET21c, to generate pET-Mus81. To express the Mus81–Mms4 complex, the *MUS81* gene was amplified from the pET-Mus81 construct above with primers 5′-ACA GCA TGC AGA TCT CGA TCC CGC GAA-3′ and 5′-TCA GCA TGC AAA AAA CCC CT-3′ (SphI). The amplified fragments were cloned into a SphI site of pET28- His$_6$-Mms4, producing pET28–His$_6$–Mms4–Mus81.

To express Rad27 (yeast Fen1) as a fusion protein (Rad27-FLAG) with a FLAG tag at its C-terminus, the *RAD27* gene was PCR-amplified using yeast genomic DNA as template with the primers; 5′-GGA ATT CAA ACA AAA AGA ACA GGG A-3′ and 5′-CCG CTC GAG TCA CTT ATC GTC ATC GTC CTT GTA GTC TCT TCT TCC CTT TGT GAC-3′ (EcoRI and XhoI). The amplified fragment was cloned into EcoRI and XhoI sites of pRS426, generating pRS426-Rad27-FLAG. The cloned fragment contained the native Rad27 promoter. To express Rad27 with a C-terminal tagged hexahistidine (Rad27-His$_6$), the *RAD27* gene was amplified with the primers; 5′-GGA ATT CAT GGG TAT TAA AGG TTT G-3′ and 5′-CCG CTC GAG TCT TCT TCC CTT TGT GAC-3′ (EcoRI and XhoI). The amplified PCR fragments were digested with EcoRI and XhoI, and cloned into pET21a cleaved with EcoRI and XhoI, resulting in pET21a-Rad27-His$_6$. All truncated forms of Rad27 were cloned into plasmid pGEX4T-1, and produced as a fusion protein with GST fused to its N-terminus. They included Rad27$_{1–366}$, Rad27$_{261–382}$, Rad27$_{261–317}$, Rad27$_{318–382}$, Rad27$_{318–350}$, Rad27$_{351–382}$ and Rad27$_{335–366}$ (the subscript indicates positions of amino acids).

Purification of Mus81–Mms4 complex and Rad27

Escherichia coli BL21-RIL cells (Stratagene) containing pET28–His$_6$–Mus81–Mms4 were grown at 37°C until A_{600} = 0.5, and expression was induced with 0.5 mM IPTG. The cells (4 l) were grown for an additional 2 h at 25°C and collected by centrifugation. Cells (7.5g, wet weight) were resuspended in 100-ml buffer A_{150} (25 mM HEPES-NaOH/pH 7.5, 10% glycerol, 0.01% NP-40, 1 mM EDTA, 1 mM dithiothreitol, 150 mM NaCl and 0.1 mM phenylmethylsulfonate). The subscript in buffer A_{150} indicates concentration of NaCl in millimoles. Cells were sonicated five times for 1 min with a 5-min cooling interval, and the lysates were centrifuged at 100 000*g* for 30 min. The resulting extract (4 mg/ml, 100 ml) was loaded onto a phosphocellulose column (5 ml, Φ 1.5 × 5 cm) equilibrated with buffer A_{150}. The column was washed with 25-ml buffer A_{150}, and proteins eluted with a linear NaCl gradient (50 ml) from 0.15 to 1 M in buffer A without DTT and EDTA. Mus81–Mms4 eluted at ~650 mM NaCl, and peak protein fractions were pooled. The pooled proteins (1.4 mg/ml, 15 ml) were incubated with Ni^{2+}–NTA beads (1 ml, Qiagen) in the presence of 10 mM imidazole for 2 h; the mixture was then poured into a column (Φ 0.7 × 5 cm), and then washed with 10-ml buffer A_{500} plus 10 mM imidazole, followed by washing with 10-ml buffer A_{500} plus 50 mM imidazole. The Mus81–Mms4 complex was eluted with buffer A_{500} plus 200 mM imidazole. Eluted peak fractions (0.38 mg/ml, 1.5 ml) were pooled, and a portion (0.25 ml) was subjected to glycerol gradient centrifugation (5 ml, 15–35% glycerol in 25 mM HEPES-NaOH/pH 7.5, 500 mM NaCl, 0.01% NP40) at 45 000 r.p.m. for 24 h in a Beckman SW55Ti rotor.

For purification of the Rad27-His$_6$ protein, *E. coli* BL21-RIL cells (2 l) harboring pET21-Rad27-His$_6$ were

grown at 37°C until the A_{600} = 0.5, followed by the addition of 0.5 mM IPTG to induce protein expression. The cells were incubated for an additional 4 h at 25°C, and then harvested. The resulting cell pellet (4.5 g, wet weight) was resuspended in 65-ml buffer A_{100} without DTT and EDTA. Crude extracts were prepared as described above for Mus81–Mms4. The extract (3.2 mg/ml, 65 ml) was loaded onto a 1.5-ml Ni^{2+}–NTA (Φ 1 × 5 cm) column, followed by successive washings with 10-ml buffer A_{100} and 10-ml buffer A_{100} plus 50 mM imidazole without DTT and EDTA. Bound proteins were eluted with buffer A_{100} plus 200 mM imidazole. The peak protein fractions (0.42 mg/ml, 15 ml) were pooled and loaded onto a Heparin column (1 ml, Φ 0.7 × 5 cm) equilibrated with buffer A_{100}. The column was then washed with 10-ml buffer A_{200}, and bound proteins eluted with buffer A plus 500 mM NaCl. Half (0.25 ml) of the pooled fraction (1.23 mg/ml, 0.5 ml) was subjected to glycerol gradient sedimentation as described for the isolation of Mus81–Mms4. Glycerol gradient fractions obtained from the Mus81–Mms4 and Rad27 preparations were analyzed in sodium dodecyl sulfate (SDS)-PAGE, followed by Coomassie blue staining. The protein yield was quantified using bovine serum albumin (BSA) as standard (Bio-Rad).

Derivatives of GST-Rad27 fusion proteins were purified using GST-beads (Amersham Biosciences) as recommended by the manufacturer.

Nuclease assays

Standard Mus81–Mms4 nuclease assays were performed in reaction mixtures (10 µl) containing 25 mM Tris–HCl/pH 8.0, 100 mM NaCl, 10 mM $MgCl_2$, 0.2 mM DTT, 0.1 mg/ml BSA, 0.1% NP-40, 5% glycerol, 10 fmol of DNA substrates and enzyme as indicated. Reaction mixtures were incubated at 30°C for 30 min, and then deproteinized with 0.2% SDS (final concentration) and 10 µg proteinase K, followed by incubation for 10 min at 37°C. After adding 2 µl of 6X stop buffer (60 mM EDTA/pH 8.0, 40% sucrose, 0.6% SDS, 0.25% bromophenol blue and 0.25% xylene cyanol), mixtures were electrophoresed at 150 V through a 12% PAGE in 0.5× TBE (45 mM Tris, 45 mM boric acid and 1 mM EDTA). Gels were dried on a DEAE-cellulose paper (Whatman) and autoradiographed. Labeled DNA products were quantified by a Phosphorimager (Molecular Dynamics, Inc.). Rad27 nuclease assays were carried out as previously described [Kim *et. al.* (39)], except that the amount of DNA substrate used was 10 fmol. When required, Mus81–Mms4 proteins were diluted in buffer (25 mM HEPES-NaOH at pH 7.5, 500 mM NaCl, 0.25 mg/ml BSA, 0.01% NP40 and 20% glycerol), while Rad27 proteins were diluted in the same buffer but with 150 mM NaCl.

Determination of kinetics parameters

Kinetic analyses were repeated in triplicate using increasing amounts (5, 10, 25, 50, 100, 200 and 500 fmol) of a double-flap substrate prepared with oligonucleotides 5, 10 and 11 (template, upstream primer and labeled downstream primer, respectively; see Table 1 for the sequences and sizes). Reactions were carried out with 1 fmol of Rad27 and 30 fmol of Mus81–Mms4 containing 90 mM NaCl per reaction. These reaction conditions led to reliable levels of products at early time points. Reaction mixtures (20 µl) were assembled on ice, followed by preincubation on ice for 10 min. Reactions were initiated by incubation at 37°C. Aliquots were withdrawn at 8 min and then added to 4 µl of 6X stop buffer. The amount of products formed was analyzed as described above. Kinetic parameters were obtained based on the Michaelis–Menten equation. $V = d[P]/dt$, where [P] is the amount of products in nanomoles. The concentration of [P] was calculated using the equation, $[P] = I_{cleaved}/(I_{uncleaved} + I_{cleaved}) \times [S]$, where [S] is concentration of substrate used, and $I_{cleaved}$ and $I_{uncleaved}$ are band intensities of products formed and substrates left, respectively. The initial velocity was plotted against [S], and the values K_m and V_{max} were calculated by nonlinear regression using Sigma Plot (Systat Software Inc.) to avoid distortion of the experimental errors, which can occur during reciprocal transformation of the data.

Immunoprecipitation

In order to detect *in vivo* interactions between Mus81–Mms4 and Rad27, a BJ2168-Mus81-TAP strain was constructed by inserting the Mus81-TAP into its native genomic locus in BJ2168 cells (*MATa ura3-52 trp1-Δ63 leu2Δ prb1-1122 pep4-3 prc1-407 GAL2*). These cells were grown to A_{600} = 2.0–3.0 in an appropriate selective media. BJ2168-Mus81-TAP/Rad27-FLAG strains were constructed by replacing chromosomal *RAD27* with Rad27-FLAG. Cell lysates from BJ2168-Mus81-TAP/Rad27-FLAG were prepared by disrupting cells using a bead beater (Biospec product) in IP buffer (25 mM HEPES-NaOH/pH 7.5, 150 mM NaCl, 10% glycerol, 0.05% NP-40, and 1 mM PMSF). Clarified lysates were incubated with 200 µl (50% slurry) of FLAG-agarose (Sigma) at 4°C for 2 h with rocking. After a brief centrifugation, the beads were washed five times with IP buffer prior to western blot analyses with PAP or FLAG antibodies.

In vitro interactions between Mus81–Mms4 and Rad27 were carried out as follows; recombinant proteins (5 pmol of each) were mixed in IP buffer (0.1 ml), and the mixture was incubated on ice for 1 h. Polyclonal Rad27 antibodies and protein-A agarose beads (5 µl each) were added and the mixture was incubated at 4°C for 2 h with rocking. After incubation, beads were collected by centrifugation, and washed eight times with IP buffer (0.5 ml for each wash), followed by western blot analyses with anti-His antibodies.

GST-pull-down assay

For the purification of GST-Rad27 and its derivatives, *E. coli* BL21-RIL cells harboring plasmids (pGEX4T-1-$Rad27_{X–Y}$, where X and Y indicate the amino acids present in the Rad27 truncated fragment) were grown at 37°C to an A_{600} of 0.5: Protein expression was induced with 1 mM IPTG for 4 h at 25°C. Cells were

harvested and resuspended in lysis buffer (25 mM HEPES-NaOH/pH 7.5, 10% glycerol, 0.01% NP-40, 150 mM NaCl and 0.1 mM PMSF). Lysates were then mixed with 0.1 ml glutathione-agarose beads (Amersham Biosciences) and the mixtures incubated at 4°C for 1 h. The GST-agarose beads were collected by centrifugation, and washed once with lysis buffer (1 ml) plus 1 M NaCl and once with lysis buffer (1 ml). The amount of GST-Rad27 bound to beads was quantified using BSA as standard (Bio-Rad) in a Coomassie-stained 10% SDS-polyacrylamide gel. Beads containing 100 pmol of GST-Rad27 were mixed with 1 pmol of Mus81–Mms4 in binding buffer (25 mM HEPES-NaOH/pH 7.5, 10% glycerol, 0.01% NP-40, 150 mM NaCl), and then incubated at 4°C for 1 h. Beads were then collected by centrifugation, washed eight times with IP buffer (0.5 ml each time), and then subjected to 10% SDS–PAGE for immunoblotting with anti-His monoclonal antibodies. When necessary, GST-Rad27 was eluted from the GST beads with 20 mM glutathione to the beads.

RESULTS

Multi-copy expression of MUS81–MMS4 suppresses lethality of dna2 helicase mutant

Previously, we showed that overexpression of Mph1 rescued the lethality of *dna2K1080E* (34), a mutant allele that abolished the helicase activity of Dna2 (35). We noted that the helicase domains of Mph1 and FancM shared some homology at their N-terminal region (36). In addition, the C-terminal region of FancM contained amino acid sequences that are conserved in ERCC4 and Mus81 family of endonucleases (17). This raised the possibility that Mph1 and Mus81 may function together to play a role similar to that of FancM. This possibility was supported by our finding that the protein–protein interaction was detected between Mph1 and Mus81 with yeast two hybrid assays (data not shown). We then assumed that Mus81 was very likely to interact functionally with Dna2 like Mph1. To test this possibility, we examined the ability of Mus81–Mms4 to suppress the lethality of *dna2K1080E* mutant in a manner similar to that observed with Mph1. For this purpose, we constructed multi-copy plasmids expressing Mus81 and Mms4, individually and in combination, under the control of their native promoters. As shown in Figure 1, transformants expressing one of the two proteins or both significantly suppressed the lethality of *dna2K1080E*. Expression of either Mus81 (MUS81) or Mms4 (MMS4) alone also resulted in significant suppression of *dna2K1080E*. The extent of suppression by the Mus81–Mms4 complex (MUS81–MMS4) was nearly as efficient as that observed with overexpression of the large subunit of RPA (RFA1, positive control; ref. 31), whereas an empty vector control (none) failed to do so.

Purification of recombinant Mus81–Mms4 complex and Rad27

To gain insight into the mechanism by which Mus81–Mms4 suppressed the *dna2* helicase mutation, we purified the Mus81–Mms4 complex as described in 'Materials and Methods' section and investigated whether it could affect the endonuclease activities of either Dna2 or Fen1. The Mus81–Mms4 complex and two forms of Rad27 (Rad27-His_6, Rad27 with a hexahistidine tag at its C-terminus; GST-Rad27, Rad27 with a GST tag at its N-terminus) were purified to near homogeneity (>95%, Figure 1B). They were devoid of nonspecific nuclease activities that interfered with our nuclease assays (see below). GST-Rad27 had virtually no endonuclease activity, whereas Rad27-His_6 possessed wild-type-like activity (data not shown). This is consistent with the observation that the N-terminal regions of Fen1 were critical to the formation of its catalytic site (37).

The purified recombinant Mus81–Mms4 complex was active and cleaved a variety of substrates, including those containing a 3′F, RF, RLe and nHJ structures (Figure 1C). We noted that Mus81–Mms4 displayed a marked sigmoidal response to the level of enzyme added. Cleavage products were hardly observed with <5 fmol of Mus81–Mms4, whereas saturation levels of cleavage products were formed with 10 fmol or more of the enzyme produced (Figure 1D). The cleavage products migrated similarly in the polyacrylamide gel used in this study. The cleavage of the labeled strands in these substrates produced largely 20-nt (with the 3′F substrate) or 22-nt long ssDNA products (with all the other substrates), indicating that the cleavage had occurred 5 nt away from nicks present in each substrate (data not shown). We also tested other substrates including a 5′F. Y-structure, intact Holliday junction and RF (RLa), and found that the Mus81–Mms4 complex poorly or hardly cleaved these substrates; the RLa substrate was weakly (100-fold less than the RLe substrate) cleaved (data not shown), while others were hardly cleaved. These findings are in keeping with the substrate specificity determined in the previous reports (14,38).

Mus81–Mms4 stimulates endonuclease activity of Rad27

Since other multi-copy suppressors of *dna2* mutants like Mgs1, Mph1 or Vts1 markedly stimulated the endonuclease activity of either Dna2 or Rad27 or both (34, 39,40), we decided to examine whether Mus81–Mms4 was able to stimulate the nuclease activities of Rad27 and Dna2. For this purpose, we first tested the ability of Mus81–Mms4 to stimulate Fen1 activity using 5′DF substrate with a 5′ 13- and 3′ 1-nucleotide flap, a physiological substrate for Fen1 (41). When reaction mixtures containing fixed levels (0.2 and 1 fmol) of Rad27 were supplemented with increasing amounts (15, 30, 60 or 120 fmol) of Mus81–Mms4, there was a marked stimulation of Rad27-catalyzed cleavage of the 5′DF substrate (Figure 2A). With 0.2 fmol of Rad27 alone, virtually no cleavage products were formed (Figure 2A, lane 3). However, the addition of Mus81–Mms4 markedly stimulated Rad27 activity (Figure 2A, compare lanes 3 and 4–7). We observed an ~12-fold stimulation by Mus81–Mms4 at higher levels of Rad27 (1 fmol) (Figure 2A, lanes 8–12). In the absence of Rad27, no cleavage products were detected even with the highest level (120 fmol) of Mus81–Mms4 (Figure 2A,

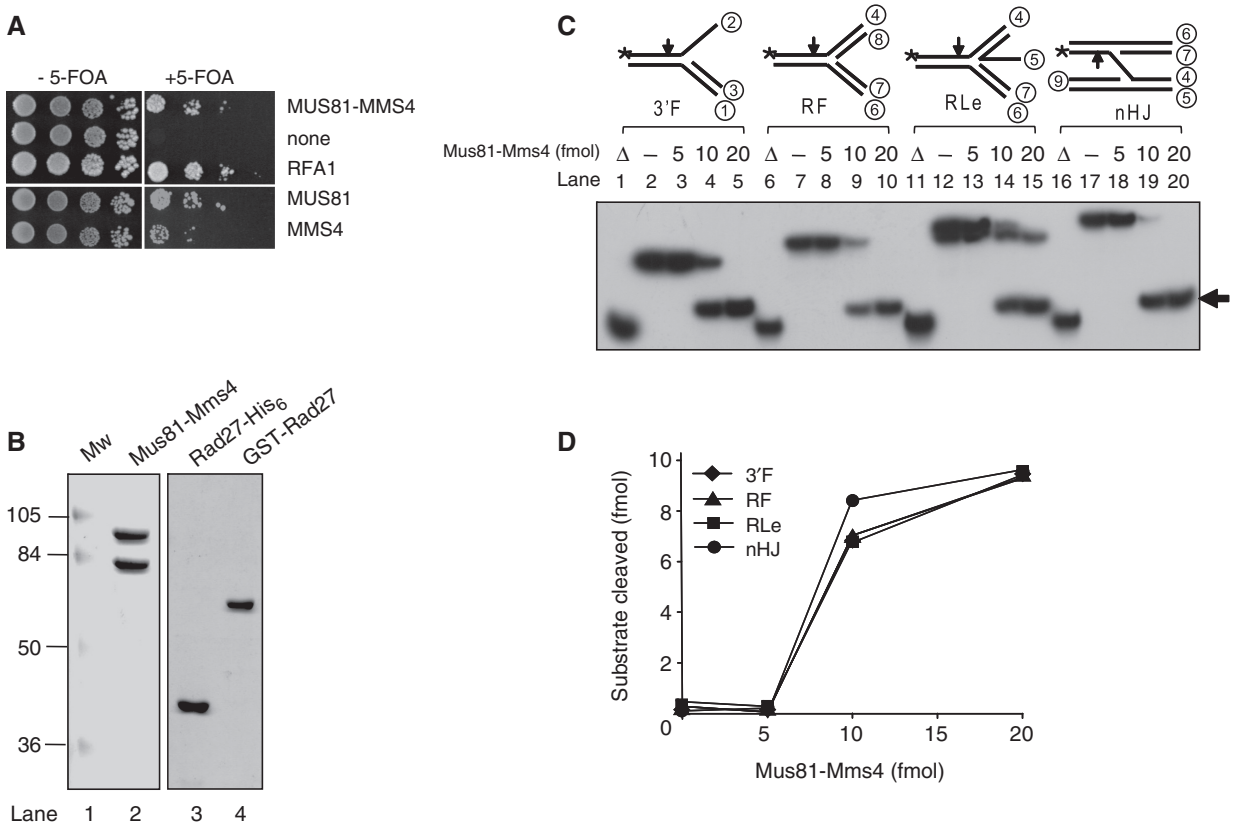

Figure 1. (**A**) suppression of *dna2K1080E* by multi-copy expression of Mus81–Mms4. The *dna2Δ* strain harboring pRS316-*DNA2* and pRS314-*dna2K1080E* was transformed with pRS325-*MUS81/MMS4* (MUS81–MMS4), pRS325 (Vector, vector only control), or pRS325-*RFA1* (RFA1, positive control). Transformants were grown on SD-Leu-Trp-His plates. Drop-dilution assays were carried out in 10-fold serial dilutions (10^4, 10^3, 10^2 and 10^1 cells) and spotted on SD-Leu-Trp-His plates in the absence (–5-FOA) or presence (+5-FOA) of 5-fluoroorotic acid. Cells were grown at 30°C for 3 days. (**B**) Purification of recombinant Mus81–Mms4 and Rad27 proteins. SDS–PAGE analysis of purified Mus81–Mms4, Rad27-His_6 and GST-Rad27 proteins. Mus81–Mms4 (1.6 μg, lane 2), Rad27-His_6 (1.4 μg, lane 3) and GST-Rad27 (1.4 μg, lane 4) were subjected to a 10% SDS–PAGE analysis, followed by Coomassie blue staining. Mw, molecular weight marker. (**C**) Cleavage of four different DNA substrates by purified Mus81–Mms4. Reactions were carried out in standard reaction mixtures containing 10 fmol of each substrate as described in 'Materials and Methods' section. The substrates tested included 3′F, 3′ flap; RF, replication fork; RLe, regressed leading-strand replication fork; nHJ, nicked Holliday junction. The structure of each substrate is schematically illustrated at the top of the autoradiograph, and oligonucleotides used to construct the DNA substrates are indicated by encircled numbers (Table 1). Increasing amounts (5, 10 and 20 fmol) of Mus81–Mms4 were added to reaction mixtures that were incubated for 30 min at 30°C. Reactions were terminated with 0.2% SDS, 10 μg proteinase K, followed by incubation for 15 min at 37°C. The products were subjected to a 12% PAGE in 0.5× TBE at 150 V. The arrows on each substrate indicate the sites of cleavage. Asterisk indicates the position of ^{32}P-labels at 5′ DNA ends. Open triangle indicates boiled substrate control. Minus sign indicates no enzyme control. (**D**) The amount (fmol) of cleavage product formed in (C) was plotted against the amounts of Mus81–Mms4 used.

lane 13), in keeping with the stringent substrate specificity of Mus81–Mms4. We also analyzed the products formed in a high-resolution gel, and noted no changes in the cleavage site of Fen1 (data not shown). We found that Mus81–Mms4 also stimulated the 5′ to 3′ exonuclease activity of Rad27 when a nicked duplex substrate was used (data not shown). In conclusion, these findings indicate that Mus81–Mms4 is able to stimulate the activity of Rad27 without altering its specificity.

Subsequently, we performed a time-course experiment with a fixed amount of Rad27 in the absence and presence of Mus81–Mms4. The rate of products formed by Rad27 (1 fmol) in the presence of Mus81–Mms4 (30 fmol) was 10- to 20-fold greater than that measured in its absence (Figure 2B and C). Mus81–Mms4 alone was totally inactive (Figure 2B, lane 3). Considering that elevated levels of Fen1 resulted in suppression of *dna2* mutations (42), our findings that the Mus81–Mms4 complex stimulated the activity of Rad27 could explain why Mus81–Mms4 suppressed a *dna2* mutation when expressed in a multi-copy plasmid (see below for further discussion). We also discovered that Mus81–Mms4 stimulated the endonuclease activity of Dna2, but weakly (2- to 3-fold at most) (data not shown). Thus, we could not rule out the possibility that the weak stimulation of Dna2 by Mus81–Mms4 could partially contribute to the suppression of the *dna2* mutation.

Effect of Mus81–Mms4 on the kinetic parameters of the Rad27 cleavage

We next determined the reaction kinetic parameters, K_m and V_{max}, as described in 'Materials and Methods' section. The addition of Mus81–Mms4 resulted in a significant increase (~2.5-fold) in V_{max} (and thus k_{cat}), and a reduction (~4-fold) of K_m (Table 2). Thus, the catalytic

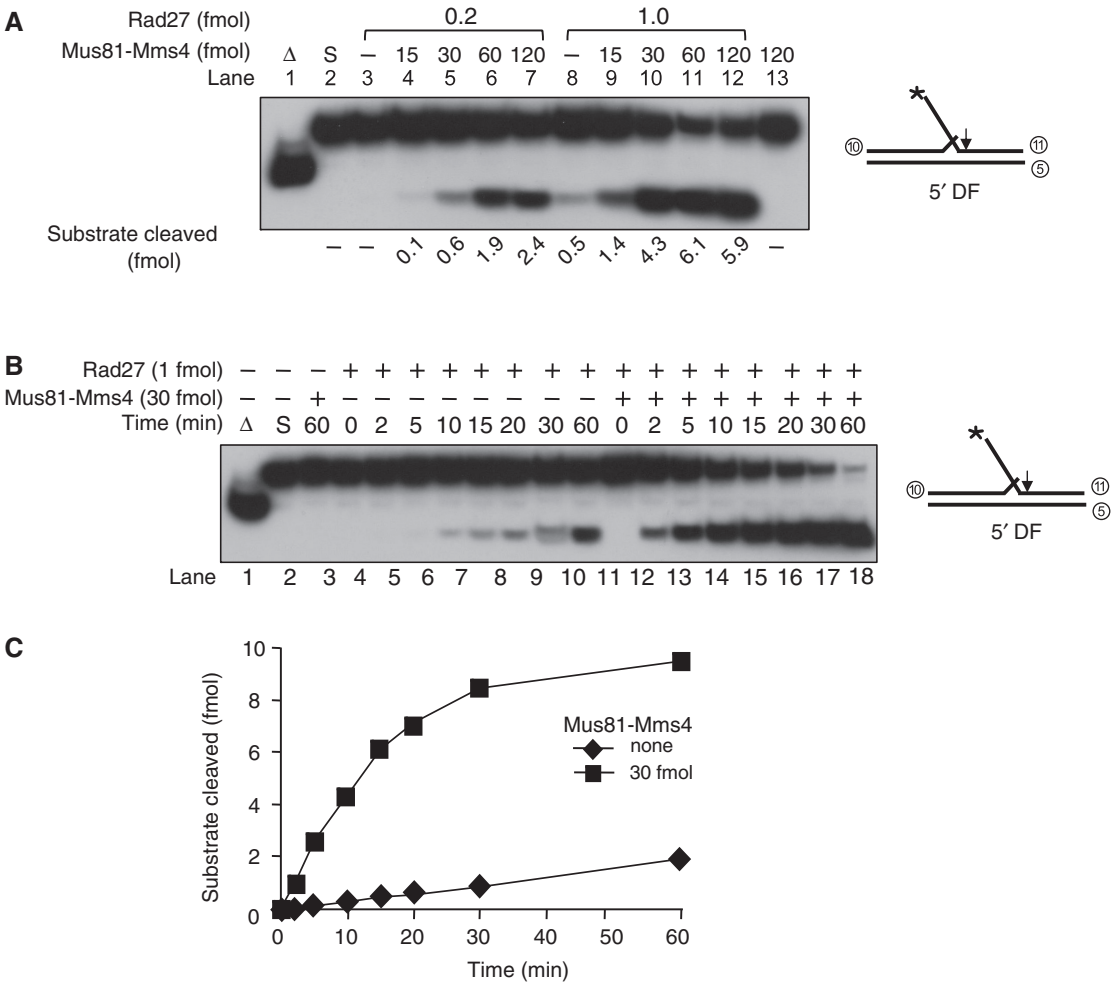

Figure 2. The Mus81–Mms4 complex stimulates the endonuclease activity of Rad27. (**A**) Standard reactions for Rad27 were carried out with two different levels (0.2 or 1 fmol) of Rad27 in the presence of increasing amounts (15, 30, 60 and 120 fmol) of Mus81–Mms4. Reaction mixtures contained 25 mM Tris–HCl/pH 8.0, 2 mM $MgCl_2$, 2 mM DTT, 0.25 mg/ml BSA and 10 fmol of the 5′DF substrate. The schematic structure of the substrate is as shown, and oligonucleotides used to construct the substrate are indicated by encircled numbers (Table 1). The reaction mixtures, after addition of indicating enzyme levels, were incubated for 15 min at 37°C. Reactions were terminated with 0.2% SDS, 10 μg proteinase K, followed by an additional incubation for 15 min at 37°C. The reaction products were analyzed similarly as described in Figure 1C. The arrows on the substrates indicate sites of cleavage. Asterisk indicates the position of ^{32}P-labels at 5′ DNA ends. Open triangle indicates boiled substrate control. S, substrate only control. (**B**) A time-course experiment of Rad27 endonuclease activity in the absence (–) or presence (+, 30 fmol) of Mus81–Mms4. The reaction mixtures containing the 10 fmol of 5′DF substrates were added with 1 fmol of Rad27, and the mixtures were incubated for varying periods as indicated. The cleavage products were analyzed in a native 10% polyacrylamide gel. (**C**) The amount (fmol) of cleavage products formed in (B) was plotted against incubation time.

Table 2. Kinetic parameters for Rad27 endonuclease activity in the presence of Mus81–Mms4

	V_{max} (nM/s × 10^{-3})	K_m (nM)	k_{cat} (s^{-1} × 10^{-2})	k_{cat}/K_m (s^{-1} M^{-1} × 10^7)
Rad27 alone	3.64 ± 0.75	25.33 ± 5.51	7.28 ± 1.49	0.30 ± 0.08
Rad27+Mus81/Mms4	9.58 ± 2.96	5.96 ± 3.10	19.17 ± 5.91	3.47 ± 0.82

efficiency (k_{cat}/K_m) of Rad27 increased markedly (~11-fold) in the presence of Mus81–Mms4 (Table 2). The increase in V_{max} suggests that the protein–protein interaction between Mus81–Mms4 and Rad27 may induce conformational change in Rad27, which in turn leads to an increased rate of catalysis. The decrease in K_m may reflect the fact that Mus81–Mms4 stabilizes the binding of Rad27 to the substrate and contributes to its increased affinity for DNA substrates. The two kinetic parameters determined suggest that the mechanism by which Mus81–Mms4 stimulates Rad27 activity could be similar to the mechanism by which PCNA stimulates the activity of Rad27. It was shown that PCNA increased V_{max} 2-fold, but decreased K_m ~12 fold of Rad27 (43). It has been postulated that the direct physical interaction of PCNA with Fen1 leads to the tethering of Fen1 at

DNA cleavage site and contributes to the increased affinity of Fen1 for DNA substrates.

Rad27 stimulates Mus81–Mms4 cleavage activity

Since genetic analyses revealed that *rad27* was synthetically lethal with either *mus81* or *mms4* (33), we tested the alternative possibility that Rad27 might affect the Mus81–Mms4 endonuclease activity. To confirm this possibility, we incubated the 3′F substrate with two different levels (2.5 and 5 fmol) of Mus81–Mms4 in the presence of increasing amounts (0–200 fmol) of Rad27 (Figure 3A). As expected from substrate specificity, the 3′F substrate was not cleaved by Rad27 (200 fmol; Figure 3A, lanes 11 and 20). In addition, the levels (2.5 and 5 fmol) of Mus81–Mms4 alone hardly produced cleavage products (Figure 3A, lanes 3 and 12) in keeping with the results as shown in Figure 1D. In the presence of Rad27, however, the 3′F substrate was efficiently cleaved by Mus81–Mms4 (Figure 3A and B). In the presence of 2.5 and 5 fmol of Mus81–Mms4, more than 20 fmol of Rad27 was required for detectable levels of cleavage products (Figure 3A, lanes 8 and 16). The cleavage reaction plateaued in the presence of more than 100 fmol of Rad27 (Figure 3A and B). We also examined the Rad27 stimulation of the Mus81–Mms4 cleavage activity using three other substrates, RF, RLe and nHJ. Like the 3′F substrate, cleavage of these substrates by Mus81–Mms4 increased in a Rad27-dependent manner (data not shown). Our data suggest that Rad27 stimulated Mus81–Mms4 regardless of substrates used. In addition, Rad27 did not alter the sites cleaved by Mus81–Mms4. The high-resolution gel analyses showed that identical products were formed in reactions containing Mus81–Mms4 and those also containing Rad27 (data not shown).

Rad27 stimulates Mus81–Mms4 in a single catalytic cycle

In order to investigate whether Rad27 stimulates Mus81–Mms4 at physiological salt concentrations, we decided to determine concentrations of NaCl for optimal cleavage of the 3′F substrate by Mus81–Mms4. Prior to this, we examined the effect of Mg^{2+} on the Fen1-mediated stimulation of Mus81–Mms4. In the absence of Mg^{2+}, cleavage did not occur (Figure 4A, lanes 2–4). We noted that increases in Mg^{2+} concentrations (2.5–10 mM) caused gradual decrease in cleavage efficiencies of 3′F DNA by Mus81–Mms4 alone (Figure 4A, compare lanes 5, 8, 11 and 14). In contrast, the addition of Rad27 (25 or 100 fmol) allowed Mus81–Mms4 to overcome the inhibitory effect of increasing concentrations of Mg^{2+}, resulting in a marked increase in the cleavage of 3′F substrate by Mus81–Mms4. Higher concentrations of $MgCl_2$ caused more robust stimulation of Mus81–Mms4 by Fen1; at 2.5 mM $MgCl_2$, stimulation was weak (<2-fold) with Rad27 added (Figure 4A, lanes 5–7). At 7.5 or 10 mM $MgCl_2$, however, the addition of 100 fmol of Rad27 resulted in more robust cleavage of the substrate

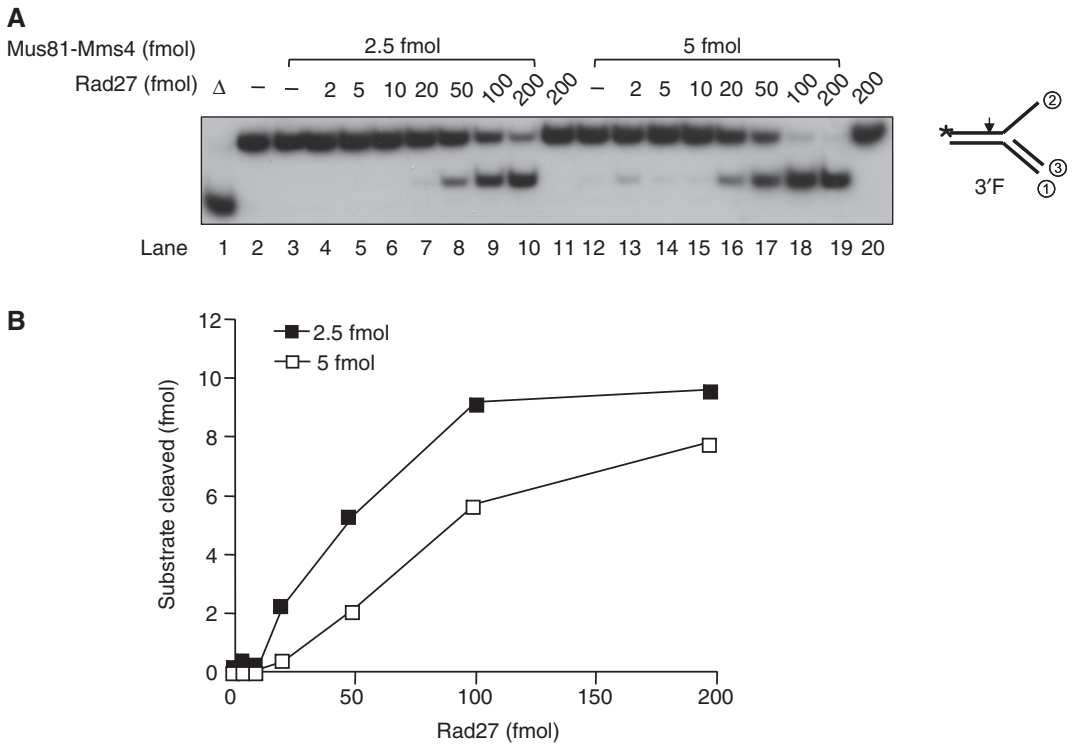

Figure 3. Rad27 stimulates the endonuclease activity of Mus81–Mms4. (**A**) Standard endonuclease assays for Mus81–Mms4 were carried out with the enzyme levels as indicated. Two levels of Mus81–Mms4 (2.5 and 5 fmol) were used in the presence of increasing amounts of Rad27 as indicated. DNA substrate used was the 3′F substrate (10 fmol) and the mixtures were incubated for 30 min at 30°C. Lanes 11 and 20 are the controls with Rad27 alone carried out independently with the same amounts of enzymes. (**B**) The amount (fmol) of cleavage products formed in (A) was plotted against the amount of Rad27 used.

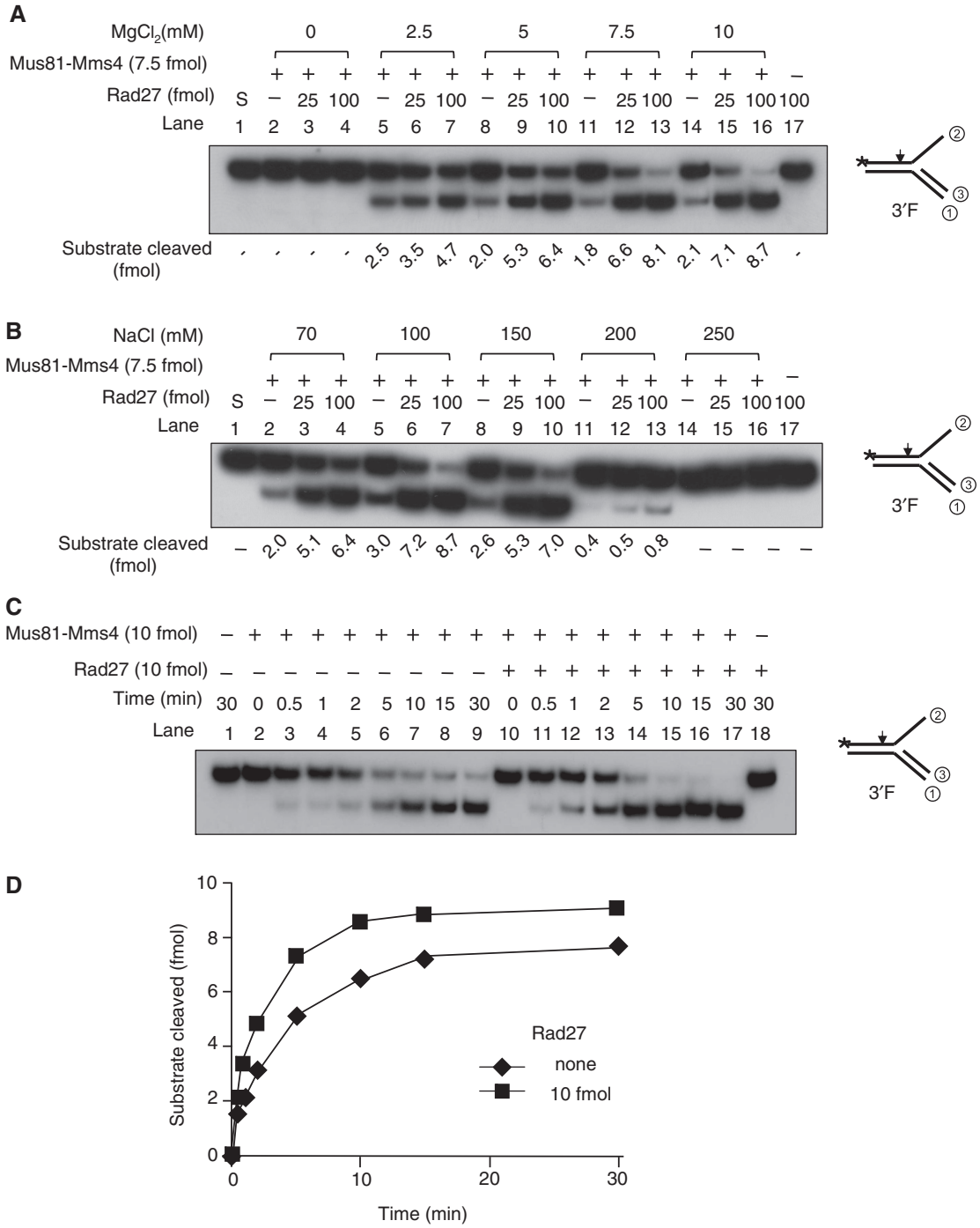

Figure 4. Rad27 stimulates Mus81–Mms4 at physiological salt concentrations. For all experiments, the 3′F substrate (10 fmol) was used. (**A**) Mus81–Mms4 stimulation by Rad27 was examined in standard reaction mixtures in increasing concentrations (2.5, 5, 7.5 and 10 mM) of $MgCl_2$. The reactions contained 7.5 fmol of Mus81–Mms4 with two different levels (25 or 100 fmol) of Rad27 as indicated. (**B**) The standard reactions in (**A**) were repeated in the presence of increasing concentrations (70, 100, 150, 200 and 250 mM) of NaCl. (**C**) A time-course experiment was performed with Mus81–Mms4 equimolar with DNA substrate (10 fmol each) in the presence of 100 mM NaCl. The reactions were carried out in the presence (+) and in the absence of Rad27 (10 fmol). The reaction mixtures were incubated at 30°C and aliquots of the reaction mixtures were withdrawn at indicated times. The cleavage products were analyzed as described in Figure 2. (**D**) The amounts of cleavage products obtained in (C) were plotted against incubation time.

(Figure 4A, lanes 11–16). This result demonstrates that effective stimulation of Mus81–Mms4 activity by Rad27 requires higher concentrations (>5 mM) of $MgCl_2$. Thus, we decided to use 10 mM $MgCl_2$ hereafter.

We also investigated whether Rad27 is able to stimulate Mus81–Mms4 at physiological salt concentrations. For this purpose, we tested varying concentrations (70, 100, 150, 200 and 250 mM) of NaCl (Figure 4B) with a fixed

concentration (10 mM) of $MgCl_2$. Mus81–Mms4 activity was hardly affected by addition of NaCl up to 150 mM, but significantly inhibited by >200 mM NaCl (Figure 4B, compare lanes 2, 5, 8 and 11). We found that Mus81–Mms4 activity was stimulated by Fen1 under all NaCl concentrations tested. Besides, the extents of Mus81–Mms4 stimulation by Rad27 were similar in the range of 70–150 mM NaCl, confirming that stimulation of Mus81–Mms4 by Rad27 can occur at the physiological salt concentration.

One potential mechanism by which Rad27 stimulates Mus81–Mms4 activity is the nonspecific DNA binding activity of Rad27 that helps dissociate Mus81–Mms4 from cleavage products, thereby rapidly recycling Mus81–Mms4. To exclude this possibility, we examined the effect of Rad27 on Mus81–Mms4 in the presence of a stoichiometric amount with the 3′F substrate DNA. If stimulation were due to the nonspecific DNA binding activity of Rad27, stimulation by recycling of Mus81–Mms4 could be minimized when all the substrates were occupied with Mus81–Mms4. For this reason, we preincubated the 3′F substrate and Mus81–Mms4 (equimolar), followed by addition of Mg^{2+} (with or without Rad27) to initiate reaction. Under this condition, marked stimulation could not be expected due to the use of a high level of Mus81–Mms4 with respect to the level of substrate. As shown in Figure 4C, we carried out a time-course experiment with reaction mixtures containing equimolar amounts (10 fmol each) of Mus81–Mms4 and 3′F substrate in the absence (Figure 4C, lanes 2–9) and presence (10 fmol; Figure 4C, lanes 10–17) of Rad27. We found that Rad27 was still able to stimulate Mus81–Mms4 activity (Figure 4C and D) more efficiently with shorter incubation period of reaction. Therefore, this result supports the notion that Rad27 stimulates Mus81–Mms4 via a specific protein–protein interaction and the stimulation occurs during a single catalytic cycle (see also below).

When we examined the cleavage products in a high-resolution gel, we found that the substrate specificity as well as the cleavage products formed by both enzymes remained identical, the same as that produced by each enzyme alone. For example, Rad27 stimulated endonuclease activity of Mus81–Mms4 with all DNA substrates tested to a similar extent, indicating that the presence of Rad27 did not alter substrate specificity of Mus81–Mms4 (data not shown). Analyses of cleavage products by a high-resolution sequencing gels revealed that the cleavage sites were not altered (data not shown).

Rad27 interacts directly with Mus81–Mms4

The marked mutual stimulation observed between Rad27 and Mus81–Mms4 prompted us to examine their physical interaction. To this end, we prepared cell-free extracts containing epitope-tagged Mus81-TAP and/or Rad27-FLAG and one of the two tagged proteins was immunoprecipitated with either PAP or anti-FLAG monoclonal antibodies (Figure 5A). Immunoprecipitation of Rad27-FLAG with anti-FLAG beads precipitated Mus81 as well (Figure 5A, lane 5). We noted that expression of Mus81-TAP was inhibited by expression of Rad27-FLAG (Figure 5A, compare lanes 2 and 3). This might account for some background observed in control in the absence of Rad27 (Figure 5A, lane 4). We also attempted to confirm direct interactions between Mus81–Mms4 and Rad27 using purified proteins (Figure 5B). Mms4 and Rad27, tagged with hexahistidine residues at their N- and C-terminus, respectively, were immunoprecipiated with anti-Rad27 polyclonal antibodies. The resulting precipitates, probed with anti-His monoclonal antibodies, revealed the presence of both Mms4 (and thus Mus81) and Rad27 (Figure 5B, lane 5). Controls indicated that the coimmuneprecipitation specifically required the simultaneous presence of Rad27, Mus81–Mms4 and anti-Rad27 antibodies (Figure 5B, lanes 3, 4 and 6). Coimmunoprecipitation in the presence of DNase I did not affect the results above, indicating that the interactions between the two proteins were not due to a DNA contaminant (data not shown). Taken together, these results indicate that Rad27 and Mus81–Mms4 interact

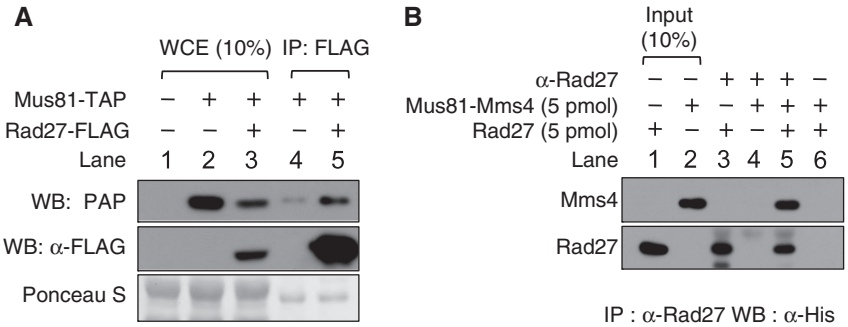

Figure 5. Rad27 interacted physically with Mus81–Mms4. (**A**) The strains that expressed either Mus81–TAP or Rad27-FLAG or both were constructed as described in 'Materials and Methods' section. Crude extracts (5.5 mg), derived from each strain as indicated at the top of figure, were mixed with anti-FLAG antibody-conjugated agarose beads (40 μl), and the mixtures were then incubated at 4°C for 2 h in binding buffer (25 mM HEPES-NaOH/pH7.5, 150 mM NaCl, 10% glycerol, 0.01% NP40). The agarose beads were collected by brief centrifugation, washed, and analyzed by western blotting using either PAP or anti-FLAG (α-FLAG) monoclonal antibodies. WCE, whole cell extract (0.25 mg); Ponceaus S indicates loading controls stained with Ponceasu S. (**B**) Recombinant Mus81–His_6Mms4 and Rad27-His_6 (5 pmol each) were mixed and incubated on ice for 1 h in buffer containing 25 mM HEPES-NaOH/pH7.5, 150 mM NaCl, 10% glycerol and 0.01% NP40. After incubation, anti-Rad27 antibodies (α-Rad27, 5 μl) and protein-A agarose (5 μl) were added to reaction mixtures, followed by an additional incubation for 1 h at 4°C with rocking. Western blot analysis was carried out with anti-His monoclonal antibodies (α-His).

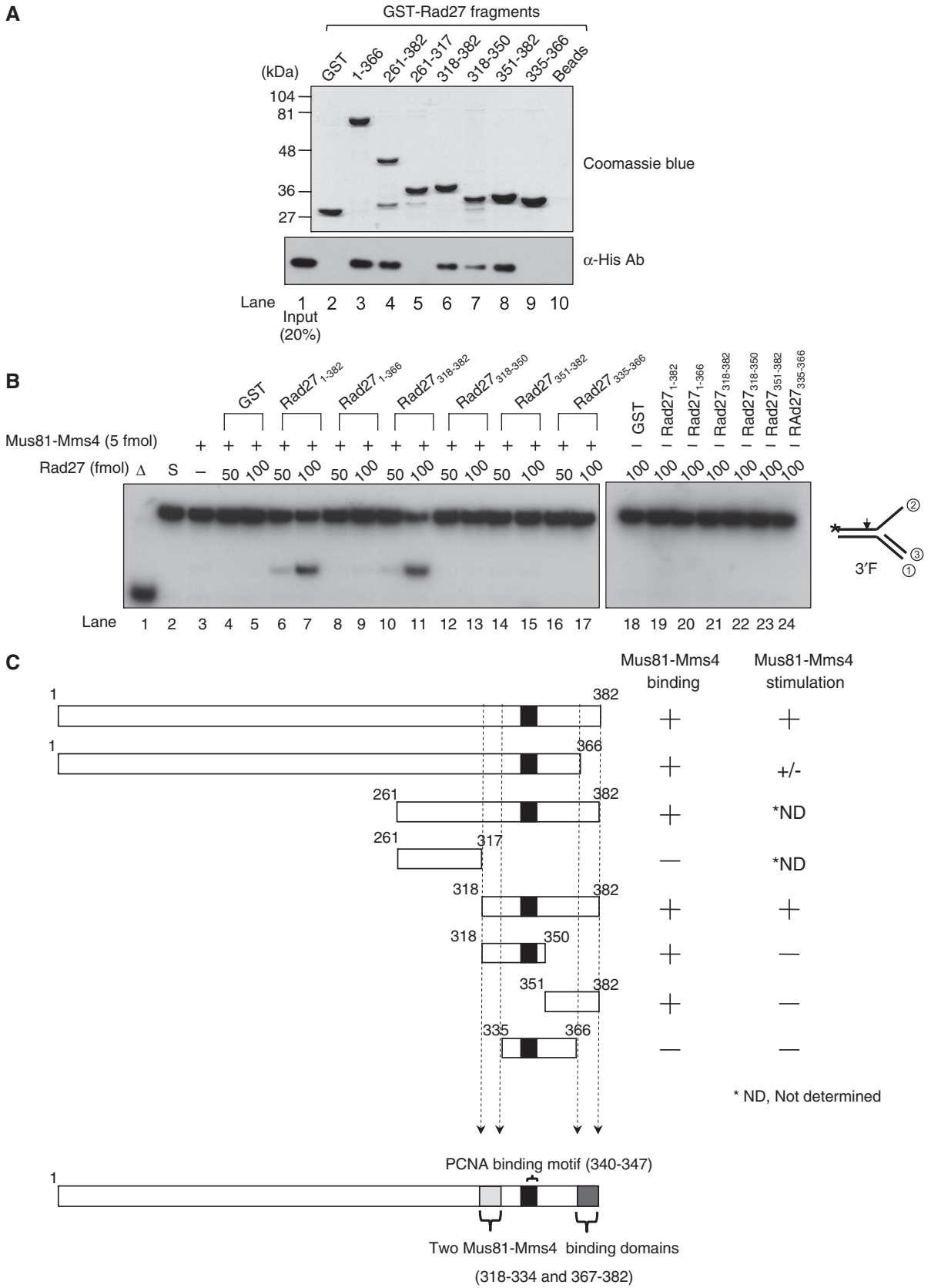

Figure 6. Mapping of specific Rad27 domains required for binding and stimulation of Mus81–Mms4 activity. (**A**) The numbers above the gel indicate amino acid positions present in the GST-fusion Rad27 derivatives. GST indicates glutathione-S transferase. Beads, Mus81–Mms4 incubated with glutathione-agarose beads in the absence of Rad27. GST-fusion Rad27 fragments bound to glutathione-agarose beads were analyzed in a 10%

continued

directly *in vivo* and suggest that their mutual activation most likely depends on this property.

Enzymatic stimulation depends on specific protein–protein interactions

The regions in Rad27 that contribute to its direct physical binding to Mus81–Mms4 were examined. For this purpose, a series of GST-fusion Rad27 fragments were prepared as described in 'Materials and Methods' section (Figure 6A, top panel, Coomassie blue), and examined for their ability to bind Mus81–Mms4 using GST-pull-down assays. The presence of Mms4-His_6 in the precipitated complexes was examined by western blot analysis with anti-His monoclonal antibodies (Figure 6A, bottom panel, α-His Ab). All of the GST-fusion Rad27 derivatives, except $Rad27_{261–317}$ and $Rad27_{335–366}$ (Figure 6A, bottom panel, lanes 5 and 9, respectively), interacted with Mus81–Mms4. GST or GST-beads alone failed to do so (Figure 6A, bottom panel, lanes 2 and 10), indicating that specific binding occurred between Rad27 fragments and Mus81–Mms4. We noted that two regions (between aa 318–334 and 367–382), flanking the known PCNA binding motif (aa 340–347), bound Mus81–Mms4 (Figure 6C). Each region alone was sufficient to bind Mus81–Mms4, since $Rad27_{318–350}$ or $Rad27_{351–382}$ interacted with Mus81–Mms4 as efficiently as $Rad27_{318–382}$ (Figure 6A, compare lanes 6–8; see also Figure 6C). It appears that the amounts of Mus81–Mms4 bound to GST-$Rad27_{318–350}$, GST-$Rad27_{318–382}$ and GST-$Rad27_{351–382}$ varied, but this is most likely due to varying levels of GST-Rad27 fragments used for the GST pull-down assays (compares lanes 6–8 in Figure 6A, bottom panel). Next, we tested whether the GST-fusion Rad27 derivatives that bound to Mus81–Mms4 were able to stimulate the enzymatic activity of Mus81–Mms4 using the 3′F substrate as shown in Figure 6B (see also Figure 6C). We found that Rad27 fragments containing only one of the two binding regions ($Rad27_{1–366}$, lanes 8 and 9; $Rad27_{318–350}$, lanes 12 and 13; $Rad27_{351–382}$, lanes 14 and 15) or none ($Rad27_{335–366}$, lanes 16 and 17) failed to stimulate the activity of Mus81–Mms4, whereas $Rad27_{318–382}$ containing both regions stimulated Mus81–Mms4 as efficiently as $Rad27_{1–382}$ (full-length) (Figure 6B, compare lanes 6and 7 to 10 and 11). Each GST-fusion Rad27 derivative did not cleave the 3′F substrate, excluding the possibility that the cleavage was due to contaminating activity derived from *E. coli* (data not shown). Thus, simultaneous presence of at least two binding motifs in Rad27 (that support the binding of Mus81–Mms4) appears to be essential for the stimulation of Mus81–Mms4 activity.

DISCUSSION

In this report, data are presented showing that the three endonucleases, Rad27, Mus81–Mms4 and Dna2, interacted genetically and functionally *in vivo* and *in vitro*. Our experimental results suggest that *MUS81–MMS4* is involved in the processing of Okazaki fragments by virtue of its genetic and functional interaction with *DNA2* and *RAD27*, both of which play critical roles in lagging strand processing. In support of this notion: (i) Overexpression of Mus81–Mms4 rescued growth defects associated with *dna2K1080E*. Furthermore, we found that *dna2-2* and *dna2-4*, the two other *dna2* mutant alleles isolated by Formosa and Nittis (44) were also suppressed by overexpression of Mus81–Mms4 (data not shown). (ii) Mus81–Mms4 and Rad27 mutually stimulated the structure-specific endonuclease activity intrinsic to each protein. (iii) Finally, the functional interactions between Rad27 and Mus81–Mms4 were shown to be mediated by specific protein–protein interactions.

We believe that suppression of *dna2* mutants by Mus81–Mms4 occurred via stimulation of Rad27. A number of previous results have shown that elevated levels of Rad27 can substitute for a functionally impaired Dna2. These include: (i) Overexpression of Rad27 suppressed several *dna2* mutant alleles, including *dna2-1* and *dna2Δ405N* (31,45). (ii) We also have shown that the *RAD27* gene can suppress *dna2K1080E* mutant (data not shown). (iii) Several suppressors of *dna2* mutations were found to stimulate the nuclease activity of Rad27. For example, *in vivo* the nonessential yeast *MGS1* gene could suppress *dna2* mutations, but *in vitro* the purified Mgs1 protein stimulated Rad27, but not Dna2 endonuclease activity (39). The observed suppression was absolutely dependent on the presence of a functional copy of *RAD27*. Thus, enhancement of Rad27 activity (or its abundance) could lead to rapid removal of flaps generated by pol δ-catalyzed displacement DNA synthesis. The net effect of this activation blocks formation of long flaps. Normally, when long flaps are formed, they could bind RPA and are efficiently cleaved by Dna2, but resistant to cleavage by Fen1 (31). Thus, enhanced or elevated levels of Rad27 activity could make cells less dependent on Dna2 activity, allowing cells to grow with impaired Dna2 activity.

Although Rad27 and Mus81–Mms4 are involved in two seemingly separate processes, their mutual stimulation described in this study suggest a more direct

Figure 6. Continued
SDS-polyacrylamide gel and stained with Coomassie blue (top gel, Commassie blue). For GST-pull-down assays (bottom gel), 1 pmol of Mus81–Mms4 was mixed with 100 pmol of GST (lane 2) or GST-fused Rad27 fragments (lanes 2–9) in binding buffer (25 mM HEPES-NaOH/pH7.5, 150 mM NaCl, 10% glycerol, and 0.01% NP40). The reaction mixtures were incubated for 1 h at 4°C with rocking. The complex formed was collected by centrifugation and washed. The presence of Mus81–Mms4 in the precipitated materials was determined by western blotting using anti-His monoclonal antibodies against His_6-Mms4 (α-His Ab, bottom panel). Lane 1 contained 0.2 pmol of Mus81–Mms4 as an input control. (**B**) The reaction mixtures contained a fixed amount (5 fmol) of Mus81–Mms4, and the reactions were carried out with 10 fmol of the 3′F substrate and two levels (50 or 100 fmol) of GST-fused Rad27 fragments using standard reaction condition as described in 'Materials and Methods' section. The cleavage products formed from the 3′ F substrates were analyzed as described in Figure 2B. (**C**) A schematic summary of the results obtained in (A) and (B). The numbers in each fragment indicate the positions of amino acids present in full-length Rad27.

interfunctional role between the two structure-specific endonucleases. Based upon the genetic and biochemical interactions between Rad27 and Mus81–Mms4, a model can be proposed that may account for how they collaborate in repairing unprocessed flaps. All flaps may not be correctly processed for a variety of reasons. For example, the two critical processing enzymes, Dna2 and Fen1, may not be able to process efficiently flaps that form a structure. Failure in processing such flaps could result in formation of double strand breaks in replicated lagging strand, which are supposed to be resected by the MRX complex to generate 3′ ssDNA overhang. The 3′ overhang then would start homologous recombination by invading replicated sister chromatid DNA, resulting in formation of recombination intermediates that are toxic to cells unless resolved. They can be normally removed by Mus81–Mms4 or Sgs1–Top3. The choice between the two pathways is governed by the availability of nicks in the recombination intermediates. Thus, processing of resilient Okazaki fragments could be ultimately assisted by Mus81–Mms4 when nicks are present in the recombination intermediates or by Sgs1–Top3 when all nicks are sealed (46).

The joint role of Rad27 and Mus81–Mms4 could come into effect via the interconversion between DNA structures specific for each endonuclease that arise from reannealing of flaps to the template DNA. It should be noted that numerous structural intermediates, called 'equilibrating flaps' (double-flap DNA with both 5′ and 3′ flaps of varying length) can result from the reannealing of flaps. These intermediates are not cleaved by either Rad27 or Mus81–Mms4 until they convert into a structural form susceptible to cleavage by each enzyme. The 5′ or 3′ flap can be converted into a 3′ or 5′ flap, respectively, in a manner similar to that seen in Holliday junction migration. If the equilibrating flaps are trapped in a structure suitable for the action of each endonuclease, they could be processed more effectively and rapidly if the two enzymes involved could stimulate each other's activity. This could constitute a feedforward and feedback stimulatory mechanism, increasing the rate of flap removal. Although BLM (47) and Mph1 (34) could directly stimulate Fen1, they are able to migrate Holliday junctions. Therefore, it is conceivable that the two helicases could contribute to Okazaki fragment processing by facilitating conversion of the equilibrating flaps into a specific structure that can be cleaved by one of the two enzymes. One example is that Sgs1 drives the annealing process to completion by virtue of its ability to displace the downstream strand. The product formed by this reaction would contain a 5′ ssDNA flap that is a substrate for Fen1. Other helicase may reverse this process to generate 3′ flap, structure that can be processed by Mus81–Mms4. Recently, the human BLM helicase was shown to stimulate nuclease activity of the Mus81–Eme1 complex (47). In addition, Rad54 was found to strongly stimulate Mus81–Mms4 in an ATP-independent fashion in humans and yeasts (48). This is interesting, considering that both BLM and Rad54 are capable of mediating the migration of branched DNA structures. Alternatively, a nuclease(s) that can simultaneously process both 5′ and 3′ double flaps could reduce the length of both flaps, and generate more rapidly a DNA substrate that can be processed by either Rad27 or Mus81–Mms4.

Although Rad27 and Mus81–Mms4 differ in their structural substrate specificity, therefore, they can act jointly to remove flap structures more efficiently particularly with aid of other protein factors that facilitate inter-conversion of substrate DNA.

The mutual stimulatory effects of Rad27 and Mus81–Mms4 also suggest that that Rad27 can play critical roles in the resolution of toxic recombination intermediates and the re-initiation of damaged RFs by activating the Mus81–Mms4 complex (see ref. 46 for details). Mus81–Mms4 is known to produce collapsed RFs, when RFs encounter damaged DNA (16,22). Then, cells attempt to repair collapsed RFs (produced by Mus81–Mms4 action) by synthesis-dependent strand annealing initiated by double-strand breaks. Therefore, the mutual stimulatory effects of Rad27 and Mus81–Mms4 provide with cells more effective means to restore damaged RFs. The collaboration between Rad27 and Mus81–Mms4/Sgs1-Top3 appears to be physiologically relevant since the synthetic-lethal interaction was detected in cells harboring mutations in *MUS81* or *SGS1* in combination with *rad27Δ* (33,49,50). This view is also in keeping with the finding that *rad27Δ* mutant was sensitive to HU, which induces replication fork arrest (51).

ACKNOWLEDGEMENTS

We thank Dr. Jerard Hurwitz for critical reading of the manuscript.

FUNDING

Funding for open access charge: National Research Foundation of Korea (Grant No. 20100000009) funded by the Ministry of Education, Science and Technology.

Conflict of interest statement. None declared.

REFERENCES

1. Cox,M.M. (2001) Historical overview: searching for replication help in all of the rec places. *Proc. Natl Acad. Sci. USA*, **98**, 8173–8180.
2. Osman,F. and Whitby,M.C. (2007) Exploring the roles of Mus81-Eme1/Mms4 at perturbed replication forks. *DNA Repair*, **6**, 1004–1017.
3. Seigneur,M., Bidnenko,V., Ehrlich,S.D. and Michel,B. (1998) RuvAB acts at arrested replication forks. *Cell*, **95**, 419–430.
4. Hickson,I.D. (2003) RecQ helicases: caretakers of the genome. *Nat. Rev. Cancer*, **3**, 169–178.
5. Chakraverty,R.K. and Hickson,I.D. (1999) Defending genome integrity during DNA replication: a proposed role for RecQ family helicases. *BioEssays*, **21**, 286–94, (review).
6. Khakhar,R.R., Cobb,J.A., Bjergbaek,L., Hickson,I.D. and Gasser,S.M. (2003) RecQ helicases: multiple roles in genome maintenance. *Trends Cell Biol.*, **13**, 493–501.
7. Heyer,W.D., Ehmsen,K.T. and Solinger,J.A. (2003) Holliday junctions in the eukaryotic nucleus: resolution in sight? *Trends Biochem Sci.*, **28**, 548–557.
8. Whitby,M.C. (2004) Junctions on the road to cancer. *Nat. Struct. Mol. Biol.*, **11**, 693–695.

9. Hollingsworth,N.M. and Brill,S.J. (2004) The Mus81 solution to resolution: generating meiotic crossovers without Holliday junctions. *Genes Dev.*, **18**, 117–125.
10. Mullen,J.R., Kaliraman,V., Ibrahim,S.S. and Brill,S.J. (2000) Requirement for three novel protein complexes in the absence of the Sgs1 DNA helicase in *Saccharomyces cerevisiae*. *Genetics*, **157**, 103–118.
11. Boddy,M.N., Gaillard,P.H., McDonald,W.H., Shanahan,P., Yates,J.R. and Russell,P. (2001) Mus81-Eme1 are essential components of a Holliday junction resolvase. *Cell*, **16**, 537–548.
12. Kaliraman,V., Mullen,J.R., Fricke,W.M., Bastin-Shanower,S.A. and Brill,S.J. (2001) Functional overlap between Sgs1-Top3 and the Mms4-Mus81 endonuclease. *Genes Dev.*, **15**, 2730–2740.
13. Fabre,F., Chan,A., Heyer,W-.D. and Gangloff,S. (2001) Alternate pathways involving Sgs1/Top3, Mus81/Mms4, and Srs2 prevent formation of toxic recombination intermediates from single-stranded gaps created by DNA replication. *Proc. Natl Acad. Sci. USA*, **99**, 16887–16892.
14. Bastin-Shanower,S.A., Fricke,W.M., Mullen,J.R. and Brill,S.J. (2003) The mechanism of Mus81-Mms4 cleavage site selection distinguishes it from the homologous endonuclease Rad1-Rad10. *Mol. Cell. Biol.*, **23**, 3487–3496.
15. Ciccia,A., Constantinou,A. and West,S.C. (2003) Identification and characterization of the human mus81-eme1 endonuclease. *J. Biol. Chem.*, **278**, 25172–25178.
16. Whitby,M.C., Osman,F. and Dixon,J. (2003) Cleavage of model replication forks by fission yeast Mus81-Eme1 and budding yeast Mus81-Mms4. *J. Biol. Chem.*, **278**, 6928–6935.
17. Ciccia,A., McDonald,N. and West,S.C. (2008) Structural and functional relationships of the XPF/MUS81 family of proteins. *Annu. Rev. Biochem.*, **77**, 259–287.
18. Chen,X.B., Melchionna,R., Denis,C.M., Gaillard,P.H., Blasina,A., Van de Weyer,I., Boddy,M.N., Russell,P., Vialard,J. and McGowan,C.H. (2001) Human Mus81-associated endonuclease cleaves Holliday junctions in vitro. *Mol. Cell*, **8**, 1117–1127.
19. Boddy,M.N., Lopez-Girona,A., Shanahan,P., Interthal,H., Heyer,W.D. and Russell,P. (2000) Damage tolerance protein MUS81 associates with the FHA1 domain of checkpoint kinase Cds1. *Mol. Cell. Biol.*, **20**, 8758–8766.
20. Abraham,J., Lemmers,B., Hande,M.P., Moynahan,M.E., Chahwan,C., Ciccia,A., Esser,J., Hanada,K., Chahwan,R., Khaw,A.K. *et al.* (2003) EME1 is involved in DNA damage processing and maintenance of genomic stability in mammalian cell. *EMBO J.*, **22**, 6137–6147.
21. Fu,Y. and Xiao,W. (2003) Functional domains required for the Saccharomyces cerevisiae Mus81-Mms4 endonuclease complex formation and nuclear localization. *DNA Repair*, **2**, 1435–1447.
22. Doe,C.L., Ahn,J.S., Dixon,J. and Whitby,M.C. (2002) Mus81-Eme1 and Rgh1 involvement in processing stalled and collapsed replication forks. *J. Biol. Chem.*, **277**, 32753–32759.
23. McPherson,J.P., Lemmers,B., Chahwan,R., Pamidi,A., Migon,E., Matysiak-Zablocki,E., Moynahan,M.E., Essers,J., Kanaar,K.R., Jasin,M. *et al.* (2004) Involvement of mammalian MUS81 in genome integrity and tumor suppression. *Science*, **304**, 1822–1826.
24. Watt,P.M., Louis,E.J., Borts,R.H. and Hickson,I.D. (1995) Sgs1: a eukaryotic homolog of E. coli RecQ that interacts with topoisomerase II in vivo and is required for faithful chromosome segregation. *Cell*, **81**, 253–260.
25. Watt,P.M., Hickson,I.D., Borts,R.H. and Louis,E.J. (1996) SGS1, a homologue of the Bloom's and Werner's syndrome genes, is required for maintenance of genome stability in Saccharomyces cerevisiae. *Genetics*, **144**, 935–945.
26. Sinclair,D.A., Mills,K. and Guarente,L. (1997) Accelerated aging and nucleolar fragmentation in yeast sgs1 mutants. *Science*, **277**, 1313–1316.
27. Myung,K., Datta,A., Chen,C. and Kolodner,R.D. (2001) SGS1, the Saccharomyces cerevisiae homologue of BLM and WRN, suppresses genome instability and homeologous recombination. *Nat. Genet.*, **27**, 113–116.
28. Liu,Y., Kao,H.I. and Bambara,R.A. (2004) Flap endonuclease 1: a central component of DNA metabolism. *Annu. Rev. Biochem.*, **73**, 589–615.
29. Burgers,P.M. (2009) Polymerase dynamics at the eukaryotic DNA replication fork. *J. Biol. Chem.*, **284**, 4041–4045.
30. Garg,P. and Burgers,P.M. (2005) DNA polymerases that propagate the eukaryotic DNA replication fork. *Crit. Rev. Biochem. Mol. Biol.*, **40**, 115–128.
31. Bae,S.H., Bae,K.H., Kim,J.A. and Seo,Y.S. (2001) RPA governs endonuclease switching during processing of Okazaki fragments in eukaryotes. *Nature*, **412**, 456–461.
32. Ii,M. and Brill,S.J. (2005) Roles of SGS1, MUS81, and RAD51 in the repair of lagging-strand replication defects in *Saccharomyces cerevisiae*. *Curr. Genet.*, **48**, 213–225.
33. Tong,A.H., Evangelista,M., Parsons,A.B., Xu,H., Bader,G.D., Pagé,N., Robinson,M., Raghibizadeh,S., Hogue,C.W., Bussey,H. *et al.* (2001) Systematic genetic analysis with ordered arrays of yeast deletion mutants. *Science*, **294**, 2364–2368.
34. Kang,Y.H., Kang,M.J., Kim,J.H., Lee,C.H., Cho,I.T., Hurwitz,J. and Seo,Y.S. (2009) The MPH1 gene of Saccharomyces cerevisiae functions in Okazaki fragments processing. *J. Biol. Chem.*, **284**, 10376–10386.
35. Bae,S.H., Choi,E., Lee,K.H., Park,J.S., Lee,S.H. and Seo,Y.S. (1998) Dna2 of Saccharomyces cerevisiae possesses a single-stranded DNA-specific endonuclease activity that is able to act on double-stranded DNA in the presence of ATP. *J. Biol. Chem.*, **273**, 26880–26890.
36. Meetei,A.R., Medhurst,A.L., Ling,C., Xue,Y., Singh,T.R., Bier,P., Steltenpool,J., Stone,S., Dokal,I., Mathew,C.G. *et al.* (2005) A human ortholog of archaeal DNA repair protein Hef is defective in Fanconi anemia complementation group M. *Nat. Genet.*, **37**, 958–963.
37. Hwang,K.Y., Baek,K., Kim,H.Y. and Cho,Y. (1998) The crystal structure of flap endonuclease-1 from Methanococcus jannaschii. *Nat. Struct. Biol.*, **5**, 707–713.
38. Ehmsen,K.T. and Heyer,W.D. (2008) Saccharomyces cerevisiae Mus81-Mms4 is a catalytic, DNA structure-selective endonuclease. *Nucleic Acids Res.*, **36**, 2182–2195.
39. Kim,J.H., Kang,Y.H., Kang,H.J., Kim,D.H., Ryu,G.H., Kang,M.J. and Seo,Y.S. (2005) In vivo and in vitro studies of Mgs1 suggest a link between genome instability and Okazaki fragment processing. *Nucleic Acids Res.*, **33**, 6137–6150.
40. Lee,C.H., Shin,Y.K., Phung,T.T., Bae,J.S., Kang,Y.H., Nguyen,T.A., Kim,J.H., Kim,D.H., Kang,M.J. and Bae,S.H. (2010) Involvement of Vts1, a structure-specific RNA-binding protein, in Okazaki fragment processing in yeast. *Nucleic Acids Res.*, **38**, 1583–1595.
41. Kao,H.I., Henricksen,L.A., Liu,Y. and Bambara,R.A. (2002) Cleavage specificity of Saccharomyces cerevisiae flap endonuclease 1 suggests a double-flap structure as the cellular substrate. *J. Biol. Chem.*, **277**, 14379–14389.
42. Budd,M.E. and Campbell,J.L. (1997) A yeast replicative helicase, Dna2 helicase, interacts with yeast FEN-1 nuclease in carrying out its essential function. *Mol. Cell. Biol.*, **17**, 2136–2142.
43. Tom,S., Henricksen,L.A. and Bambara,R.A. (2000) Mechanism whereby proliferating cell nuclear antigen stimulates flap endonuclease 1. *J. Biol. Chem.*, **275**, 10498–10505.
44. Formosa,T. and Nittis,T. (1999) Dna2 mutants reveal interactions with Dna polymerase alpha and Ctf4, a Pol alpha accessory factor, and show that full Dna2 helicase activity is not essential for growth. *Genetics*, **151**, 1459–1470.
45. Budd,M.E., Choe,W.C. and Campbell,J.L. (1995) DNA2 encodes a DNA helicase essential for replication of eukaryotic chromosomes. *J. Biol. Chem.*, **270**, 26766–26769.
46. Kang,Y.H., Lee,C.H. and Seo,Y.S. (2010) Dna2 on the road to Okazaki fragment processing and genome stability in eukaryotes. *Crit. Rev. Biochem. Mol. Biol.*, **45**, 71–96.
47. Zhang,R., Sengupta,S., Yang,Q., Linke,S.P., Yanaihara,N., Bradsher,J., Blais,V., McGowan,C.H. and Harris,C.C. (2005) BLM helicase facilitates Mus81 endonuclease activity in human cells. *Cancer Res.*, **65**, 2526–2531.
48. Matulova,P., Marini,V., Burgess,R.C., Sisakova,A., Kwon,Y., Rothstein,R., Sung,P. and Krejci,L. (2009) Cooperativity of

Mus81·Mms4 with Rad54 in the resolution of recombination and replication intermediates *J. Biol. Chem.*, **284**, 7733–7745.

49. Loeillet,S., Palancade,B., Cartron,M., Thierry,A., Richard,G.F., Dujon,B., Doye,V. and Nicolas,A. (2005) Genetic network interactions among replication, repair and nuclear pore deficiencies in yeast. *DNA Repair*, **4**, 459–468.
50. Pan,X., Ye,P., Yuan,D.S., Wang,X., Bader,J.S. and Boeke,J.D. (2006) A DNA integrity network in the yeast *Saccharomyces cerevisiae*. *Cell*, **124**, 1069–1081.
51. Lopes,J., Ribeyre,C. and Nicolas,A. (2006) Complex minisatellite rearrangements generated in the total or partial absence of Rad27/hFEN1 activity occur in a single generation and are Rad51 and Rad52 dependent. *Mol. Cell Biol.*, **26**, 6675–6689.